Experiments on Charge-Changing Collisions of Lithium Ionic and Atomic Beams*

S. K. Allison, J. Cuevas, and M. Garcia-Munoz
Enrico Fermi Institute for Nuclear Studies, University of Chicago, Chicago, Illinois
(Received July 5, 1960)

Beams of Li^+ ions accelerated to kinetic energies in the range 10–475 kev were brought into charge equilibrium in the gases H_2, He, and N_2 and the fractional amounts of Li^-, Li^0, Li^+, Li^{++}, Li^{+++} measured. Because of the relatively large amount of Li^- in an equilibrated beam below 40 kev in energy in propane and nitrous oxide, limited investigations were carried out in these gases. The anomalously large Li^{++} yield in helium at Li^7 energies below 100 kev was noted.

By holding each separated charged constituent successively in an orbit in a magnetic field, admitting gas, and observing the beam attenuation, the total cross section for all charge-changing collisions was observed. Through application of the differential equations for growth or decay of a charged component, certain individual charge-changing cross sections can be deduced from these observed sums. Values are given for $(\sigma_{\bar{1}0}+\sigma_{\bar{1}1})$, σ_{01}, σ_{10}, σ_{12}, σ_{21}, and $(\sigma_{32}+\sigma_{31})$ in H_2, He, and N_2 target gases throughout the energy range. Upper limits can be assigned to $\sigma_{0\bar{1}}$, $\sigma_{1\bar{1}}$, σ_{13}, and σ_{23}. Use of data on $\sigma_{1\bar{1}}$ in H_2 from other sources provides values of $\sigma_{0\bar{1}}$ in that gas. Values for σ_{21} for Li^{++} in helium gas, compared, at common velocities, with σ_{10} for He^+ in helium, and $\sigma_{0\bar{1}}$ for H^0 in helium, show the exchange nature of the He^+He interaction compared to that of the other isoelectronic structures.

I. INTRODUCTION

A BEAM of Li^+ ions is easily prepared by heating a paste of $Li_2O \cdot Al_2O_3 \cdot SiO_2$ in the proper proportions[1] on a hot filament and accelerating the evaporated, singly charged lithium ions electrically to the desired kinetic energy. When such an ion beam enters a gas-containing chamber, hereafter called the converter cell, inelastic collisions take place in which the charge of the moving ions is changed, by capture or loss of one or more electrons. The newly formed beam constituents in turn suffer such charge-changing collisions. After a sufficient path length in the converter cell, the beam has come to charge equilibrium, and the fractions $F_{i\infty}$ of the various charged types present is a function only of the velocity of the beam and the nature and temperature of the converter gas. Let i represent the positive charge on the beam constituent in units having the magnitude of the electronic charge. In the present experiments the fractions $F_{i\infty}/F_{1\infty}$ with $i=-1$, 2, 3, and $F_{0\infty}$ were measured in the gases H_2, He, N_2 and in some gases having polyatomic molecules.

A second aspect of the experiments dealt with the measurement of the collision cross sections for such charge changing events. The method of measurement indicated only that the charge of the moving lithium ion had been changed in the collision; it did not in itself indicate whether the event had been electron loss or capture, either single or multiple. We therefore indicate the quantity we measured as $\sum_f \sigma_{if}$, i referring, as above, to the ionic charge before the event, and f the charge after the event. By using the various charged constituents emerging from the converter cell, we measured $\sum_f \sigma_{if}$ for $i=-1$, 0, 2, 3 in H_2, He, and N_2 target gases. A special difficulty arose in trying to measure $\sum\sigma_{1f}$; in many cases it was computed from other measurements.

Measurements of this type on lithium ionic beams have been reported by various experimenters in the U.S.S.R.

Leviant, Korsunsky, Pivovar, and Podgornyi[2] have reported measurements of $F_{2\infty}/F_{1\infty}$ and $F_{3\infty}/F_{1\infty}$ for lithium beams in the kinetic energy range 85–250 kev, moving in air. Under the same conditions, they give values of σ_{12} and σ_{13}. These will be discussed in a later section of this report.

Some estimates of the velocity dependence of the lithium ion charge have been made by studying the density of ionization along the "handle" of "hammer" tracks in emulsions.[3] An extensive study of the charge fractions $F_{i\infty}$ in a lithium beam equilibrated by passage through a thin celluloid film has appeared.[4] The kinetic energies used in these experiments covered the range 0.58–5.2 Mev.

A research group led by Fogel[5] has published results of experiments on $\sigma_{1\bar{1}}$, the cross section for the simultaneous capture of two electrons by Li^+. They performed experiments in the target gases H_2, Ar, and Kr. Only upper limits for this cross section were obtained in our work; they will be compared with the results of Fogel *et al.* in a later section of this report. The experiments of Fogel *et al.* covered the kinetic energy range from 5 to 50 kev.

The kinetic energy range, in terms of Li^7, in the present work was from 10 to 475 kev. In the upper part of the range, Li^6 was sometimes used as the beam constituent, but it was assumed that Li^6 and Li^7 would have identical behavior if moving with the same velocity, and the result was expressed in terms of Li^7. Although, as previously remarked, the immediate result

* This work was supported in part by the U. S. Atomic Energy Commission.

[1] J. P. Blewett and G. J. Jones, Phys. Rev. **50**, 465 (1936).

[2] Kh. L. Leviant, M. I. Korsunsky, L. I. Pivovar, and I. M. Podgornyi, Proc. Acad. Sci. U.S.S.R. **103**, 3, 403 (1955).

[3] M. I. Kuznetsov, P. I. Lukirsky, and N. A. Perfilov, Doklady Akad. Nauk S.S.S.R. **100**, 665 (1955).

[4] Ya. A. Teplova, I. S. Dmitriev, V. S. Nikolaev, and L. N. Fateeva, J. Exptl. Theoret. Phys. (U.S.S.R.) **32**, 974 (1957) [translation: Soviet Phys.-JETP **5**, 797 (1957)].

[5] Ya. M. Fogel, V. F. Kozlov, A. A. Kalmykov, and V. J. Murator, J. Exptl. Theoret. Phys. (U.S.S.R.) **36**, 1312 (1959) [translation: Soviet Phys.-JETP **36**(9), 929 (1959)].

of a cross-section measurement by the method employed is $\sum_f \sigma_{if}$, in many cases it is possible to deduce individual σ_{if} cross sections from this sum by combining the cross section and $F_{i\infty}$ results in the analysis. A few experiments were performed to study the growth of F_1 and F_2 as the converter cell pressure was increased. These curves can also be calculated once the cross section is known. The constituent growth curves of this work will be described in another paper.[6]

II. EXPERIMENTAL METHOD AND APPARATUS

A. Preparation of the Lithium Ionic Beam

Two different accelerators were used in the course of the present experiments. The kinetic energy range 10 to 50 kev was covered by a portable acceleration tube 41 cm long, made from two sections of Pyrex glass pipe. The dc high voltage supply for the acceleration was a standard 50-kv power supply, regulated to 0.1%. The ion source used in all the experiments has been previously illustrated.[7] The kinetic energy range 75–475 kev was covered by our Cockcroft-Walton accelerator, or "kevatron." The Li^+ ion beams varied widely in intensity during the many months of data taking. Before passing through the defining apertures in the converter cell, which were 0.091 cm in diameter and 20.6 cm apart,[8] the Li^7 beam was usually in the range 3–20 microamperes. After the fine apertures, Li^+ currents of 10^{-8} to 10^{-7} ampere were usual in the Faraday cell detector. In spite of the most careful lining up of the various apertures, it was often necessary to obtain the final, small, beam adjustment by positioning a permanent magnet outside the beam tube.

In all the measurements, the ion beam leaving the accelerator tube was magnetically analyzed before passing into the converter cell (see Fig. 2). If the vacuum was good in the acceleration tube, the lithium beam was remarkably clean, containing only the two Li isotopes, with the largest other component a peak of relative intensity 0.05 at mass 23, which was probably Na^+ but could have been LiO^+. The magnetic resolution used was always sufficient to remove this component and with the magnet used in the 75–475 kev range the two Li isotopes were easily separated. The isotopic separation was not complete in the smaller magnet used for the 10–50 kev range.

In the upper energy ranges the measurements were taken with Li^6, since it has the higher velocity, and is more easily magnetically deviable for the same energy. For this purpose separated Li^6 was used in the ion source material.

B. Measurement of the Equilibrated Beam Constituents $F_{i\infty}$

Experimental problems in the $F_{i\infty}$ measurements have previously been discussed by Allison.[9] The problems relevant to the detectors arise from the fact that the relative intensities of ionic beams differing in charge must be measured, and one must either use a different detector for each magnetically separated beam or, if one charged beam detector is used, and the ionic beam alternately guided to it magnetically, the detector response and beam intensity must be independent of magnetic field. The estimation of the Li^0 constituent is a separate problem and was done calorimetrically.

All $F_{i\infty}$ measurements on charged beams were carried out using a Faraday chamber, thus obviating the difficulties of calibrating secondary electron detectors. The inside dimensions of the chamber were 1.58-cm diameter by 6.4 cm long; the beam entering it had a diameter of 0.2 cm. A thick steel housing protected it from stray magnetic fields, and bias curves of the current measured as a function of the potential difference between the chamber and its vacuum housing showed no detectable loss of beam or secondary electrons from the entrance.

In the calorimetric detector for the neutral beam, the temperature rise of a platinum disk 0.635 cm in diameter and 2.5×10^{-3} cm in thickness was measured as it came to thermal equilibrium when hit by the beam. The thermometric element was a highly temperature sensitive resistor[10] in the form of a minute bead attached to the rear surface of the platinum. The resistance at room temperature was approximately 3000 ohms; the decrease per degree centigrade rise was about 110 ohms. The platinum disk was held in position and out of contact with the detector housing by four quartz fibers cemented to it by silver chloride. The thermistor bead was attached to the disk with a trace of Duco cement, and a fine platinum wire was also attached to the disk so that it could be used as a secondary electron detector, but only in this capacity for the location and adjustment of the beam prior to a calorimetric measurement.[11] The calorimeter was housed in thick copper to slow down any changes and eliminate spatial fluctuations in the ambient temperature. A second thermistor was embedded in the copper jacket, and the true rise in temperature was always considered to be the difference between the temperature of the detector thermistor and that of the ambient thermistor. The temperature resistance curve of each thermistor was carefully studied with an accurate mercury thermometer.

The calorimeter was placed so that the entire emergent beam from the converter cell was incident on it; then the magnet between it and the converter cell was

[6] S. K. Allison, J. Cuevas, and M. Garcia-Munoz, Rev. Sci. Instr. (to be published).

[7] S. K. Allison and C. S. Littlejohn, Phys. Rev. **104**, 959 (1956), Fig. 1.

[8] The converter cell is illustrated in Fig. 2 and described in Table II of the report of S. K. Allison, Phys. Rev. **109**, 76 (1958).

[9] S. K. Allison, Revs. Modern Phys. **30**, 1137 (1958), p. 1142 ff.

[10] Thermistor No. 32A5, Victory Engineering Corporation, Union, New Jersey.

[11] We are indebted to Mr. Walter Mankawich, Development Engineer, for the delicate operations of assembly of the calorimeter.

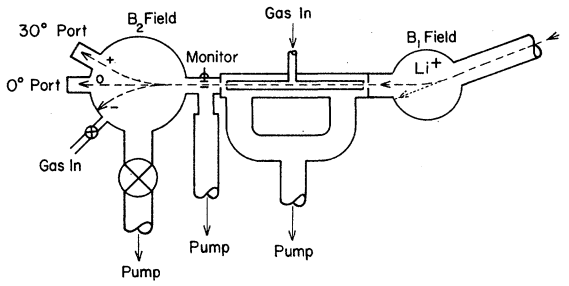

FIG. 1. Schematic drawing of apparatus, showing differentially pumped compartments, converter cell (center) and measuring chamber (left).

energized, thus subtracting the charged beams. At the lower kinetic energies, the temperature rises were less than 10°C, and a linear relation between the watts input from the beam and the temperature rise could be assumed. At the higher kinetic energies, the increasing radiation efficiency disturbed the linearity and it was necessary to measure the watts input versus temperature rise curve by changing the beam intensity at constant kinetic energy. The secondary electron emission current of the disk was a reliable indicator of relative beam current when all other factors were unchanged.

As implied by the notation, $F_{i\infty}$ indicates the fractional number of ions or atoms of charge $i|e|$ in the moving beam after it has traversed sufficient target gas so that each individual F_i remains unchanged on further traversal. In measuring a charged beam constituent, such as Li^-, Li^{++}, or Li^{+++}, the "B_2 field" magnet (Fig. 1) was set to direct the desired constituent into the Faraday cell at the 30° port. With full pumping speed in the B_2 field compartment, and the Li^+ beam traversing the converter cell, gas was admitted to the converter cell and the rise of intensity of the selected beam constituent was observed in the Faraday chamber. The rate of rise of the constituent (other than Li^+) decreased at higher converter cell pressures, and finally a broad maximum was attained, followed by a slow decline. The slow decline at the higher gas pressures was due to the scattering of the beam out of the detector apertures.[12] The pressure in the converter cell was set in the region of the maximum, and read on a McCleod gauge. The current to the Faraday chamber was read on a vibrating reed electrometer, and this reading, divided by i, was compared to the reading when the Li^+ constituent was directed, by a change in B_2, into the chamber. The ratio is $F_{i\infty}/F_{1\infty}$.

The pressure in the "B_2 field" compartment was also read on a second McCleod gauge to be sure that the inevitable diffusion of some of the converter cell gas into the B_2 cell had not raised the pressure to a value requiring some correction to the observed $F_{i\infty}/F_{1\infty}$ ratios. All such corrections proved to be negligible compared to the estimated ±15% over-all accuracy.

[12] The question of the amount of gas to put in the beam path to attain equilibrium for a charge constituent will be taken up in another publication [Rev. Sci. Instr. (to be published)]. Let $(pl)_{90}$ represent the product of the pressure in microns times the length of path in cm for attainment of 90% of $F_{i\infty}$ for the beam constituent i. $(pl)_{90}$ varied from 40 to 200 microns×cm for the gases H_2 and N_2. For the production of Li^{++}, helium has the very high value of 750 microns×cm at 75 kev, and in general, helium values of $(pl)_{90}$ are high.

C. Measurement of Total Cross Sections $\sum_f \sigma_{if}$

In order to measure $\sum_f \sigma_{if}$ for a charged beam other than Li^+, gas was admitted to the converter cell until the exit beam contained a sufficient amount of the desired constituent. This constituent was then magnetically directed (by the appropriate B_2 field) to the Faraday chamber at the 30° port, and its intensity noted together with the pressure in the B_2 cell, which was taken with the B_2 cell diffusion pump disconnected. By varying the B field slightly, the beam profile was explored, and any subtractable background revealed. Gas was then admitted to the B_2 cell, in sufficient amount to attenuate the beam through charge exchange to about 0.7 of its low-pressure value. The profile of the attenuated beam was examined, as before. Since, to a first approximation, for every charge changing event during the traverse of the B_2 cell an ion is lost to the detector,

$$\sum_f \sigma_{if} = -(1/\pi) \log_e R, \tag{1}$$

where R is the attenuation ratio ($R<1$), and

$$\pi = Al\xi P/RT. \tag{2}$$

l is the length of path from which ions with their charges changed are removed from the detector (approximately the diameter of the B_2 field), A is Avogadro's number, ξ is the number of atoms per molecule of the gas, P is the gas pressure in dynes/cm² in the B_2 cell, R is 8.31×10^7 ergs/mole °C, and T is the absolute temperature in the B_2 cell. Thus π is the number of gas *atoms* in a volume l cm long and 1 cm² in sectional area transverse to its length, and $\sum_f \sigma_{if}$ will be the cross section per *atom* of target gas.

TABLE I. Experimental results on equilibrium fractions of a Li^7 ionic and atomic beam traversing hydrogen gas. (Experimental error ±15% unless specially noted.)

Kinetic energy (kev)	$F_{\bar{1}\infty}/F_{1\infty}$	$F_{0\infty}$	$F_{2\infty}/F_{1\infty}$	$F_{3\infty}/F_{1\infty}$
20	1.8×10^{-5}	0.18	...	...
30	5.9×10^{-5}	...	...	...
40	9.6×10^{-5}	0.17	...	...
50	17.0×10^{-5}	0.22	9.4×10^{-5}	...
75	1.4×10^{-4}	...	3.7×10^{-4}	...
100	2.5×10^{-4}	...	14×10^{-4}	...
150	3.0×10^{-4}	0.19	5.9×10^{-3}	...
200	3.1×10^{-4}	0.20	1.4×10^{-2}	$<3\times10^{-6}$
250	4.2×10^{-4}	0.16	2.5×10^{-2}	$<2\times10^{-5}$
300	3.7×10^{-4}	0.16	3.6×10^{-2}	...
350	3.4×10^{-4}	...	$2.7^{a}\times10^{-2}$	1.8×10^{-5}
400	2.9×10^{-4}	0.09	5.0×10^{-2}	5.8×10^{-5}
475	1.8×10^{-4}	...	0.10	4.0×10^{-4}

[a] Unreliable.

Measurements of $\sum_f \sigma_{0f}$ could not be carried out using the Faraday cell detector, and were made with a secondary electron emitting detector[13] placed in the 0° port, Fig. 1. Since only intensity ratios of the same constituent are concerned, the absolute efficiency of the detector does not enter. Its reliability was verified by showing that the admission of gas into the B_2 cell did not change its reading in the absence of the magnetic field.

D. Beam Monitors

Although in many cases the lithium ion beams from the accelerators remained sufficiently constant so that detector readings uncorrected for beam variation were sufficiently reliable, often better results could be obtained by comparing all readings with those of a beam monitor. Although many schemes for monitoring the beam were tested, no one device gave satisfactory results for all the various types of measurement.

The most widely used monitor was a parallel plate ionization chamber built into the equipment at the output beam end of the converter cell. The ion current collected was proportional to the product of the beam intensity by the gas pressure in this differentially pumped compartment. In measurements of $F_{i\infty}$, where no gas was admitted into the system except the steady flow through the converter cell, this monitor, adequately shielded from changes in the magnetic field, was useful.

A wire screen monitor[14] which intercepted part of the beam was occasionally used for cross-section measurements, but not for $F_{i\infty}$ measurements where scattering from it might have changed the fractions from those typical of the gas in the converter cell.

III. RESULTS

A. Relative Intensities of Charge Components in Equilibrated Beams

The quantities directly determined by experiment were $F_{\bar{1}\infty}/F_{1\infty}$, $F_{0\infty}$, $F_{2\infty}/F_{1\infty}$, and $F_{3\infty}/F_{1\infty}$, provided the ionic ratios were above approximately 5×10^{-6}. The target gases were H_2, He, N_2, C_3H_8, N_2O. A few readings of $F_{\bar{1}\infty}/F_{1\infty}$ in NO showed little difference from those in N_2O. The results are given in Tables I–IV.

TABLE II. Experimental results on equilibrium fractions of a Li^7 ionic and atomic beam traversing helium gas. (Experimental error ±15% unless specially noted.)

Kinetic energy (kev)	$F_{\bar{1}\infty}/F_{1\infty}$	$F_{0\infty}$	$F_{2\infty}/F_{1\infty}$	$F_{3\infty}/F_{1\infty}$
50	...	...	9.4×10^{-3}	...
75	9.9×10^{-5}	...	1.3×10^{-2}	...
96	...	0.17	...	...
100	1.9×10^{-4}	...	1.8×10^{-2}	...
150	3.7×10^{-4}	0.15	2.5×10^{-2}	...
200	3.7×10^{-4}	0.16	2.9×10^{-2}	5.1×10^{-6}
250	3.8×10^{-4}	0.14	4.3×10^{-2}	2.2×10^{-5}
300	3.1×10^{-4}	0.12	3.8×10^{-2}	3.3×10^{-5}
350	4.0×10^{-4}	...	5.4×10^{-2}	1.1×10^{-4}
400	2.9×10^{-4}	0.08	7.2×10^{-2}	1.6×10^{-4}
475	2.4×10^{-4}	...	12×10^{-2}	7.2×10^{-4}

[13] See reference 9, Fig. IV-2.
[14] S. K. Allison, Phys. Rev. **110**, 670 (1958), see item M, Fig. 1.

TABLE III. Experimental results on equilibrium fractions of a Li^7 ionic and atomic beam traversing nitrogen gas. (Experimental error ±15% unless specially noted.)

Kinetic energy (kev)	$F_{\bar{1}\infty}/F_{1\infty}$	$F_{0\infty}$	$F_{2\infty}/F_{1\infty}$	$F_{3\infty}/F_{1\infty}$
20	3.5×10^{-5}	0.14	...	...
30	8.0×10^{-5}	0.16	...	...
40	15×10^{-5}	...	2.4×10^{-4}	...
50	20×10^{-5}	0.22	4.4×10^{-4}	...
75	2.0×10^{-4}	...	8.5×10^{-4}	...
100	2.7×10^{-4}	...	2.2×10^{-3}	...
150	2.7×10^{-4}	0.18	6.1×10^{-3}	...
200	2.3×10^{-4}	0.16	1.6×10^{-2}	4.9×10^{-6}
250	1.6×10^{-4}	0.13	2.9×10^{-2}	2.1×10^{-5}
300	1.3×10^{-4}	0.12	4.7×10^{-2}	5.1×10^{-5}
350	1.0×10^{-4}	...	7.4×10^{-2}	2.2×10^{-4} [a]
400	1.1×10^{-4}	0.09	12.0×10^{-2}	3.2×10^{-4}
475	7.5×10^{-5}	...	0.17	1.1×10^{-3}

[a] Unreliable reading.

TABLE IV. Experimental production of Li^- and Li^0 by equilibration in N_2O and in C_3H_8 (propane) gases. (Experimental error ±15% unless otherwise noted.)

Kinetic energy (kev)	C_3H_8 $F_{\bar{1}\infty}/F_{1\infty}$	C_3H_8 $F_{0\infty}$	N_2O $F_{\bar{1}\infty}/F_{1\infty}$
20	1.5×10^{-4}	0.22	7.1×10^{-5}
30	3.6×10^{-4}	0.28	2.2×10^{-4}
40	3.9×10^{-4}	0.23	...
50	3.8×10^{-4}	0.27	3.9×10^{-4}
75	3.4×10^{-4}	...	...
100	1.9×10^{-4}	0.26	...
150	1.5×10^{-4}	0.30	...
200	...	0.19	...
250	...	0.16	...
300	...	0.14	...

B. Total Charge-Changing Cross Sections

The cross-section sums on which measurements were taken are the values of $\sum_f \sigma_{if}$ for $i=-1, 0, 1, 2, 3$. Some of the measurements on $\sum\sigma_{1f}$ have not been given in the tables of results (Tables V–VIII) for the following reason. Throughout the kinetic energy range we have investigated, Li^+ forms by far the most abundant component of an equilibrated beam. The cross-section sum $\sum\sigma_{1f}$ is the smallest of those we attempted to evaluate by direct measurement, and, in general, the measurements could not stand up under the test that, when the same amount of gas was admitted as had been necessary for a cross-section measurement, no attenuation of the mixed beam in the absence of the magnetic field should be observable. This means that the cross sections were so low that they approach the limit measurable under our geometry, and the attenuation of the beam due to small angle Coulomb scattering was comparable to that

TABLE V. Measurements of the total cross sections for all collisions in which a Li^7 atom or ion undergoes change of charge. ($\Sigma_f \sigma_{if}$ in 10^{-17} cm² per atom of target gas.) Target gas hydrogen. (Experimental error ±15%.)

Kinetic energy (kev)	$\Sigma\sigma_{\bar{1}f}$	$\Sigma\sigma_{0f}$	$\Sigma\sigma_{2f}$	$\Sigma\sigma_{3f}$
10	90	14	···	···
20	90	16	···	···
30	88	19	···	···
40	85	22	37	···
50	80	24	42	···
75	96	···	45	···
100	80	···	60	···
150	71	17	61	···
200	57	···	59	···
250	50	···	47	102
300	53	···	35	75
350	39	9.7	32	71
400	33	···	25	35
475	33	7.2	14	38

due to charge changing. Actually in helium gas and at kinetic energies 10–30 kev the attenuation (if any) of a Li^+ beam due to charge-changing collisions was completely overshadowed by losses due to small angle scattering and no $\sum\sigma_{1f}$ could be detected. The experimental result merely set an upper limit on $\sum\sigma_{1f}$.

In the following section of this paper it is shown that, with very reasonable assumptions, one may compute $\sum\sigma_{1f}$ from the other cross section and $F_{i\infty}$ measurements, and due to the difficult scattering correction, this seems to be more accurate than an attempted direct measurement. In order to compute $\sum\sigma_{1f}$, it is necessary to measure $F_{0\infty}$. In those gases and at those kinetic energies where $F_{0\infty}$ was directly measured or could be reliably interpolated, we have not tabulated $\sum\sigma_{1f}$ measurements. The graphs of the deduced values, however, contain σ_{10} and σ_{12}, compiled from other measurements. In certain cases, notably helium at low Li^7 energies, where the very small product of flux times kinetic energy in the Li^0 beam made calorimetric determination too difficult, we have tabulated upper limits of $\sum\sigma_{1f}$ as giving the best information available, and calculated upper limits for $F_{0\infty}$ from them in the following section.

TABLE VI. Measurements of the total cross sections for all collisions in which a Li^7 atom or ion undergoes change of charge. ($\Sigma_f \sigma_{if}$ in 10^{-17} cm² per atom of target gas.) Target gas helium. (Experimental error ±15%.)

Kinetic energy (kev)	$\Sigma\sigma_{\bar{1}f}$	$\Sigma\sigma_{0f}$	$\Sigma\sigma_{1f}$	$\Sigma\sigma_{2f}$	$\Sigma\sigma_{3f}$
10	···	15	···	···	···
20	···	22	<1.3	···	···
30	···	26	<1.9	···	···
40	···	26	<2.4	···	···
45	···	26	<2.5	···	···
50	···	···	···	6.8	···
75	77	···	≲4.5	7.7	···
100	72	···	≲4.2	10.5	···
150	58	25	···	22	···
200	53	···	···	28	···
250	39	···	···	24	70
300	29	···	···	25	68
350	42	13	···	23	66
400	31	···	···	21	57
475	36	9.0	···	18	38

IV. DEDUCTIONS FROM THE EXPERIMENTAL RESULTS

A. Values of $F_{i\infty}$

Since $\sum F_{i\infty}=1$, the various $F_{i\infty}$ values may be computed from the measurements of Tables I–IV through

$$F_{1\infty}=\frac{1-F_{0\infty}}{1+(F_{\bar{1}\infty}+F_{2\infty}+F_{3\infty})/F_{1\infty}}, \tag{3}$$

TABLE VII. Measurements of the total cross sections for all collisions in which a Li^7 atom or ion undergoes change of charge. ($\Sigma\sigma_{if}$ in 10^{-17} cm² per atom of target gas.) Target gas nitrogen. (Experimental error ±15%.)

Kinetic energy (kev)	$\Sigma\sigma_{\bar{1}f}$	$\Sigma\sigma_{0f}$	$\Sigma\sigma_{2f}$	$\Sigma\sigma_{3f}$
10	···	28	···	···
20	130	31	···	···
30	130	32	···	···
40	128	33	58	···
50	122	32	78	···
75	120	···	71	···
100	123	···	56	···
150	96	26	59	···
200	93	···	50	···
250	90	···	43	91
300	103	···	41	78
350	120	31	30	55
400	82	···	29	69
475	88	26	21	48

TABLE VIII. Measurements of the total cross sections for all collisions in which a Li^7 atom or ion undergoes change of charge. ($\Sigma_f \sigma_{if}$ in 10^{-17} cm² per molecule of target gas.) Target gas propane.

Kinetic energy (kev)	$\Sigma\sigma_{\bar{1}f}$	$\Sigma\sigma_{0f}$
20	···	54
30	···	64
40	~340	73
50	···	78

in which $F_{0\infty}$ and all the ratios $F_{i\infty}/F_{1\infty}$ appearing in the right-hand member have been measured. In Figs. 2–5 the deduced $F_{i\infty}$ values are graphically displayed by drawing a smooth curve through the individual points deduced as above from the experiments.

B. Values of Individual Cross Sections

There are five differential equations (four of which are independent) which give the rate of change of the fraction of any charge component. Written in a form to

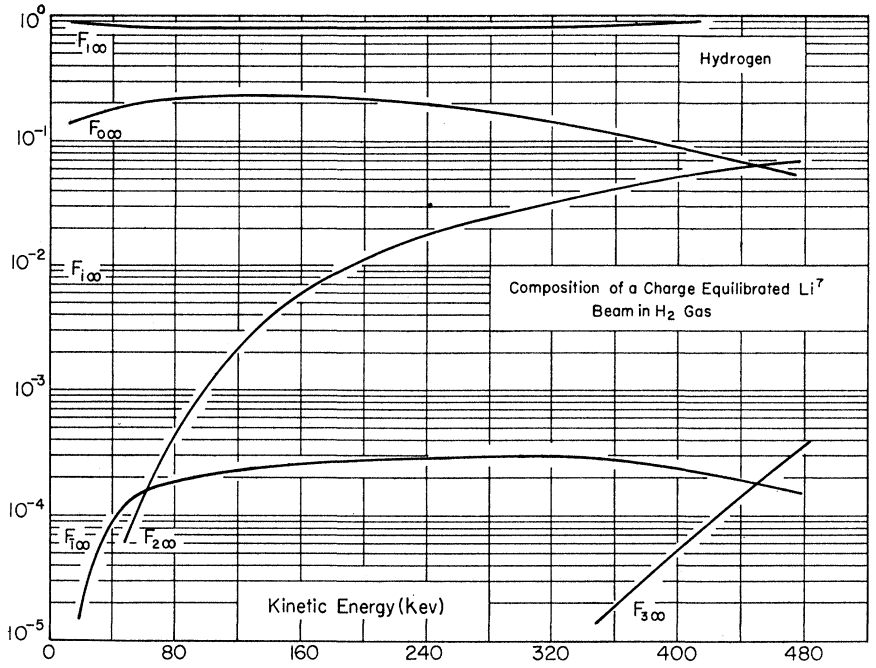

FIG. 2. Ordinates are fractions of the total beam in various charge states for a charge equilibrated lithium beam in hydrogen gas.

suit the experimental setup, in which the number of gas molecules per cm^3, represented by π, is changed in a tube of constant length, they are

$$dF_{\bar{1}}/d\pi = F_0\sigma_{0\bar{1}} + F_1\sigma_{1\bar{1}} + F_2\sigma_{2\bar{1}} + F_3\sigma_{3\bar{1}} - F_{\bar{1}}\sum\sigma_{\bar{1}f}, \quad (4)$$

$$dF_0/d\pi = F_{\bar{1}}\sigma_{\bar{1}0} + F_1\sigma_{10} + F_2\sigma_{20} + F_3\sigma_{30} - F_0\sum\sigma_{0f}, \quad (5)$$

$$dF_1/d\pi = F_{\bar{1}}\sigma_{\bar{1}1} + F_0\sigma_{01} + F_2\sigma_{21} + F_3\sigma_{31} - F_1\sum\sigma_{1f}, \quad (6)$$

$$dF_2/d\pi = F_{\bar{1}}\sigma_{\bar{1}2} + F_0\sigma_{02} + F_1\sigma_{12} + F_3\sigma_{32} - F_2\sum\sigma_{2f}, \quad (7)$$

$$dF_3/d\pi = F_{\bar{1}}\sigma_{\bar{1}3} + F_0\sigma_{03} + F_1\sigma_{13} + F_2\sigma_{23} - F_3\sum\sigma_{3f}. \quad (8)$$

In an experimental survey such as the one reported here, where the accuracy of a measurement is in general $\pm 15\%$, certain terms in the preceding equations can be safely considered as negligible.

(1) Electron loss cross sections in which two or more electrons of widely different ionization potential are stripped off in one collision, are small compared to πa_0^2 (a_0 = first Bohr orbit radius; $\pi a_0^2 = 8.8\times 10^{-17}$ cm^2). The successive ionization potentials of lithium occur in

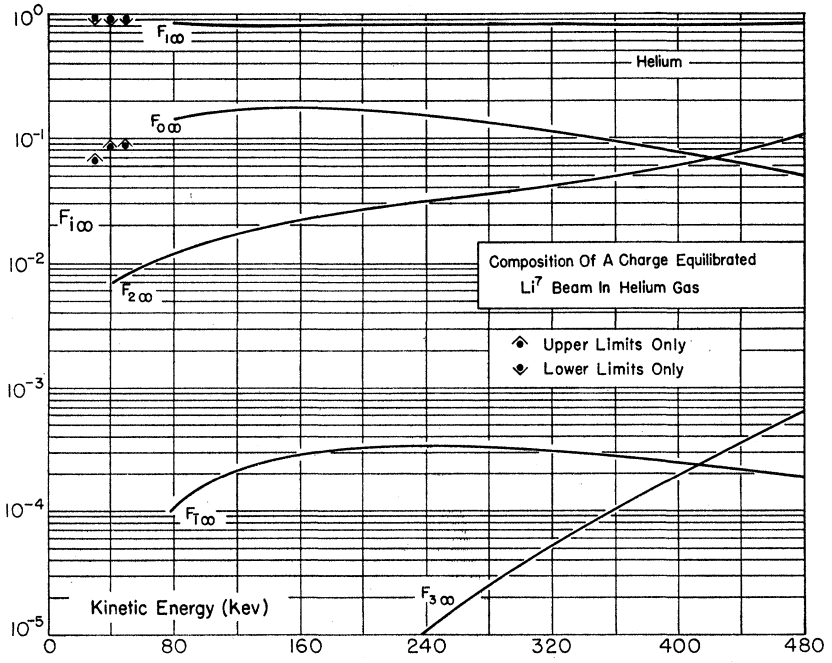

FIG. 3. Ordinates are fractions of the total beam in various charge states for a charge equilibrated lithium-7 beam moving in helium gas.

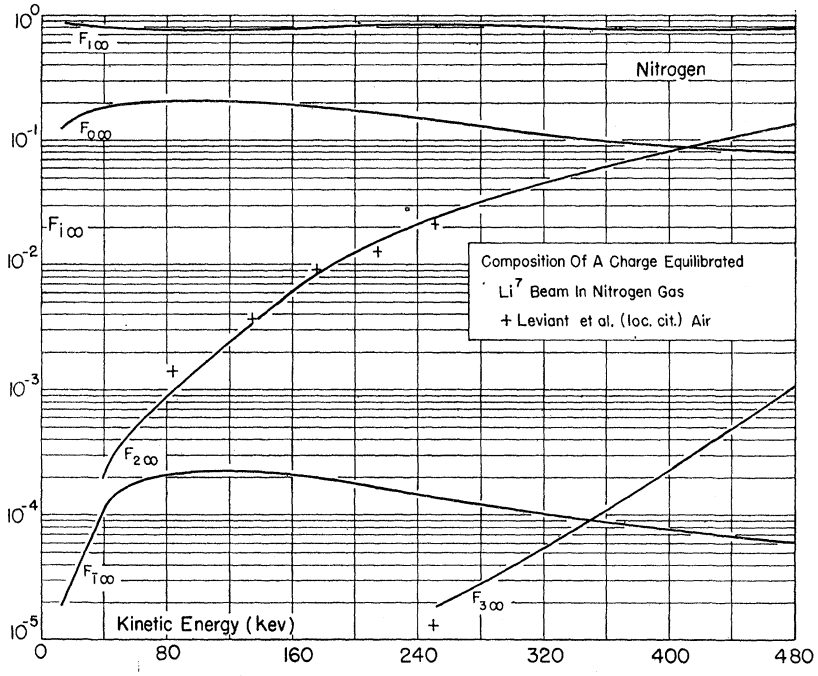

FIG. 4. Ordinates are fractions of the total beam in various charge states for a charge equilibrated lithium-7 beam moving in nitrogen gas.

wide steps:

Li^-, <1 ev; Li^0, 5.4 ev; Li^+, 75.3 ev; Li^{++}, 121.8 ev.

It is therefore considered that $\sigma_{\bar{1}3}$, σ_{03}, σ_{13}, $\sigma_{\bar{1}2}$, σ_{02} will be such small cross sections.

(2) Electron capture cross sections in which several electrons are caught, and one of these has a binding energy to lithium less than it had in the target gas molecule from which it came.

Thus we consider $\sigma_{3\bar{1}}$, σ_{30}, $\sigma_{2\bar{1}}$, σ_{20} to be small, for the present case of lithium ions, due to the low binding energy of the third (valence) electron in lithium and, *a fortiori*, that of the fourth electron in the negative ion.

Using these simplifications, we will rewrite Eqs. (4) to (8), at the same time setting the derivatives equal to zero, to represent the condition of the equilibrated beam.

Thus we obtain

$$F_{0\infty}\sigma_{0\bar{1}}+F_{1\infty}\sigma_{1\bar{1}}=F_{\bar{1}\infty}(\sigma_{\bar{1}0}+\sigma_{\bar{1}1}), \quad (9)$$

$$F_{\bar{1}\infty}\sigma_{\bar{1}0}+F_{1\infty}\sigma_{10}=F_{0\infty}(\sigma_{0\bar{1}}+\sigma_{01}), \quad (10)$$

$$F_{\bar{1}\infty}\sigma_{\bar{1}1}+F_{0\infty}\sigma_{01}+F_{2\infty}\sigma_{21}=F_{1\infty}(\sigma_{1\bar{1}}+\sigma_{10}+\sigma_{12}), \quad (11)$$

$$F_{1\infty}\sigma_{12}+F_{3\infty}\sigma_{32}=F_{2\infty}(\sigma_{21}+\sigma_{23}), \quad (12)$$

$$F_{1\infty}\sigma_{13}+F_{2\infty}\sigma_{23}=F_{3\infty}(\sigma_{32}+\sigma_{31}). \quad (13)$$

In order to proceed further with these equations, we shall introduce a third simplification, namely that there is an upper limit, perhaps not sharply defined, but certainly usable, for any single cross-section sum $\sum_f \sigma_{if}$. This idea is just as precise, and no more so, than the custom of assigning definite interaction radii to atoms and molecules in a discussion of chemical reactions in the gaseous phase. For instance, we shall assume that no lithium charge changing cross-section sum in nitrogen gas can significantly exceed that for the removal of the fourth electron in Li^-, namely, from Table VII, about 260×10^{-17} cm^2 per nitrogen molecule. For hydrogen and helium the assumed upper limits are 200×10^{-17} cm^2 and 80×10^{-17} cm^2 per molecule and per atom, respectively.

If we use this additional assumption, and the measured values in the tables, individual cross sections may be deduced from Eqs. (9) to (13). As an illustration we treat the case of Li^7 of kinetic energy 150 kev, moving in nitrogen gas.

C. Deduction of Individual Cross Sections for Li^7 Moving with 150-kev Kinetic Energy in N_2 Gas

The available numerical values are (see Fig. 4 and Table VII)

$$F_{\bar{1}\infty}=2.2\times10^{-4}, \qquad \sum\sigma_{\bar{1}f}=96,$$
$$F_{0\infty}=0.19, \qquad \sum\sigma_{0f}=26,$$
$$F_{1\infty}=0.81, \qquad \sum\sigma_{2f}=59.$$
$$F_{2\infty}=5.0\times10^{-3},$$

In the above, and in the following comments, cross sections are in units of 10^{-17} cm^2 unless explicitly stated.

Consider the term $F_{3\infty}$ $(\sigma_{32}+\sigma_{31})$ which appears in Eq. (13). Using the postulated upper limit of any total cross-section sum as 130 per nitrogen atom, and the failure to find any Li^{+++} we may state the inequality

$$F_{3\infty}(\sigma_{32}+\sigma_{31})<5.4\times10^{-4}.$$

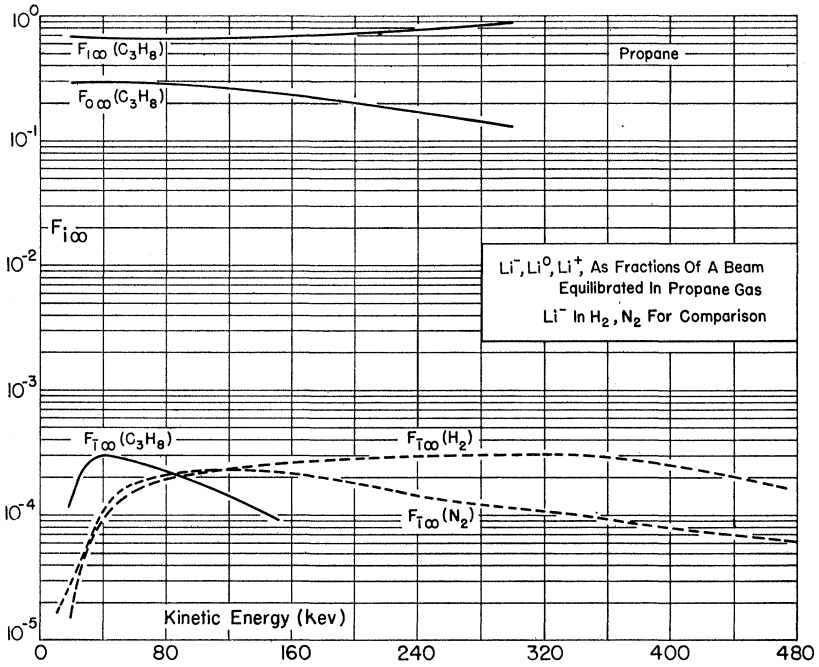

FIG. 5. Fractions of a charge equilibrated lithium-7 beam in the forms Li^-, Li^0, Li^+ in propane. For comparison, fractions of Li^- in hydrogen and nitrogen. At low kinetic energies propane is a much more efficient producer of Li^-, although the same $F_{\bar{1}\infty}$ is eventually attained, at higher Li velocities, by the other gases. $F_{0\infty}$ is also larger, at low velocities than in the elementary gases (see Figs. 2 to 4).

Thus, by alternatively entertaining the hypothesis that either σ_{13} or σ_{23} is zero, Eq. (13) permits us to establish upper limits for them, namely,

$$\sigma_{13}<6.7\times10^{-21}\text{ cm}^2;\ \sigma_{23}<0.11\times10^{-17}\text{ cm}^2.$$

Now consider Eq. (12), in which $(\sigma_{21}+\sigma_{23})$ appears. Our neglect of small cross sections means that this is just our measured quantity $\sum\sigma_{2f}$. But we have just set an upper limit for σ_{23}; accordingly, to our $\pm15\%$ accuracy

$$\sigma_{21}=59\times10^{-17}\text{ cm}^2.$$

Furthermore, it is clear that the term $F_{3\infty}\sigma_{32}$ is of negligible size compared to the others in Eq. (12), and solved for σ_{12} we obtain

$$\sigma_{12}=3.6\times10^{-18}\text{ cm}^2.$$

We can now use Eq. (9) to elicit information concerning $\sigma_{0\bar{1}}$ and $\sigma_{1\bar{1}}$. The right-hand member of this equation can be evaluated directly from the measurements, using Table VII, col. 1, and Fig. 4; its value is 2.1×10^{-2}. In this way the following upper limits are obtained:

$$\sigma_{0\bar{1}}<1.1\times10^{-18}\text{ cm}^2\quad\text{and}\quad\sigma_{1\bar{1}}<2.6\times10^{-19}\text{ cm}^2.$$

Fogel *et al.*[5] have measured $\sigma_{1\bar{1}}$ directly for Li^7 in H^2, Ar, Kr from 5 kev to 60 kev. Their values in argon should be roughly comparable to those for the N_2 molecule. At 60 kev they find $\sigma_{1\bar{1}}$ in argon to be 1×10^{-19} cm^2 and although it is rising slightly as the energy increases it is apparently close to a maximum which lies below the limit imposed by our considerations.

Finally, the upper limit we have established for $\sigma_{0\bar{1}}$ allows us to conclude, from Eq. (10), that to our postulated accuracy

$$\sigma_{01}=\sum\sigma_{0f}=26\times10^{-17}\text{ cm}^2$$

and $$\sigma_{10}=\sigma_{01}F_{0\infty}/F_{1\infty}=6.1\times10^{-17}\text{ cm}^2.$$

By following procedures close to those outlined above, a set of values in the various gases was deduced from the directly observed $\sum_f\sigma_{if}$ values. The deduced cross sections are

$$(\sigma_{\bar{1}0}+\sigma_{\bar{1}1}),\quad\sigma_{01},\quad\sigma_{10},\quad\sigma_{21},\quad\sigma_{12},\quad\text{and}\quad(\sigma_{31}+\sigma_{32}).$$

Upper limits[15] were set for the cross sections

$$\sigma_{0\bar{1}},\quad\sigma_{1\bar{1}},\quad\sigma_{13},\quad\text{and}\quad\sigma_{23}.$$

In addition, numerical relations[15] were established between $\sigma_{0\bar{1}}$ and $\sigma_{1\bar{1}}$ as follows. From Eq. (9)

$$\sigma_{0\bar{1}}+(F_{1\infty}\sigma_{1\bar{1}})/F_{0\infty}=F_{\bar{1}\infty}(\sigma_{\bar{1}0}+\sigma_{\bar{1}1})/F_{0\infty}.\qquad(14)$$

Using the numerical values of the illustrative example above, this means (σ's in units of 10^{-17} cm^2)

$$\sigma_{0\bar{1}}+4.3\sigma_{1\bar{1}}=0.026.$$

For the higher energies, where $F_{3\infty}$ and $\sum_f\sigma_{3f}$ could be measured, Eq. (13) provides a similar numerical connection between σ_{13} and σ_{23}.

If we use the measurements of Fogel *et al.*[5] on $\sigma_{1\bar{1}}$ for Li^7 in H_2 gas[16] between 5 and 60 kev, we can use Eq. (14) to obtain $\sigma_{0\bar{1}}$, remembering that $(\sigma_{\bar{1}0}+\sigma_{\bar{1}1})$ is essentially the measured quantity $\sum\sigma_{\bar{1}f}$. The results are included

[15] These upper limit tables and numerical relationships are not being presented for publication. They may be obtained by writing to the authors.

[16] We have assumed that the cross sections of Fogel *et al.* are per hydrogen molecule and divided them by two for inclusion in our data. Furthermore, we have selected those cross sections $\sigma_{1\bar{1}}$ from Fig. 1 of Fogel's paper in which the incident Li^+ beam is presumably free from ions in metastable states.

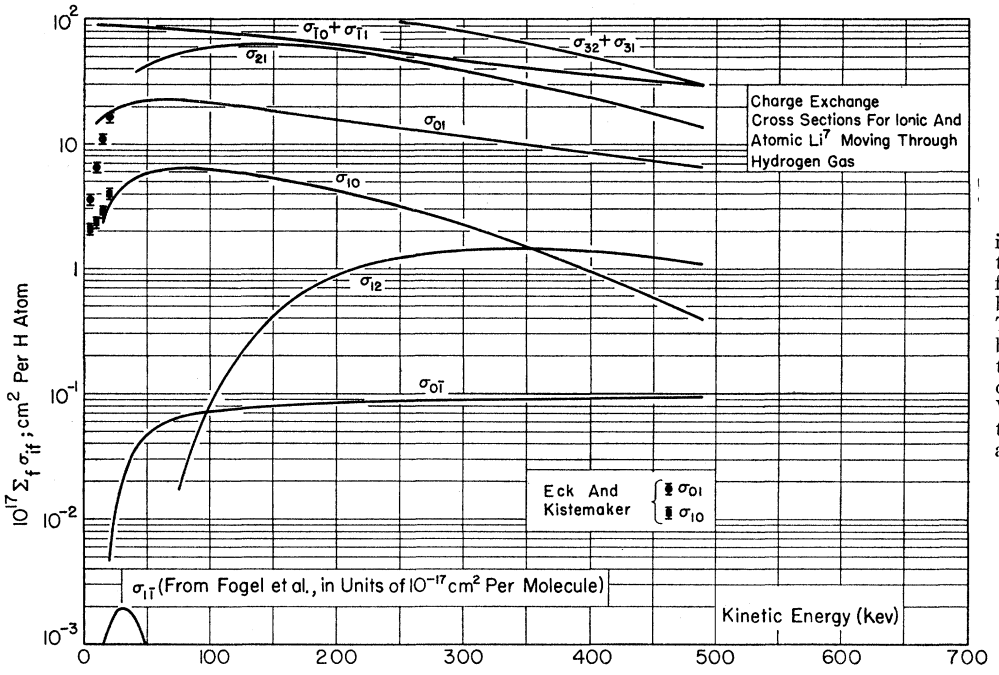

FIG. 6. Charge-changing collision cross sections in H_2 gas deduced from the sums obtained by direct measurement. The values of $\sigma_{0\bar{1}}$ have been obtained through the use of measurements of $\sigma_{1\bar{1}}$ by Fogel *et al.* Values of σ_{01} and σ_{10} due to Eck and Kistemaker are included.

in the graphical presentations of the deductions, which are shown in Figs. 6 to 8. Errors in the smooth curve values of these cross sections are roughly $\pm 15\%$.[17]

V. COMPARISON OF OUR RESULTS WITH DATA FROM OTHER EXPERIMENTERS

A. Equilibrated Beam Fractions

In the paper of Teplova *et al.*[4] the observations of Kuznetsov *et al.*[3] on rapid changes in the ion density along Li^8 tracks in emulsions are discussed. It is pointed out that the change in the effective value of Z^2 in a Li beam during moderation is not abrupt and a rapid change in slope in the blackening vs range curve is not to be expected. The most rapid rate of change of Z^2(eff) lies in the Li^7 kinetic energy range between 2 and 1 Mev, where Z^2(eff) falls from 6.2 to 3.3.

The results of Teplova *et al.* on the $F_{i\infty}$ values of Li^7 beams emerging from celluloid foils of thickness greater than 10 $\mu g/cm^2$ are shown in Fig. 9. Their data extend from about 0.58 Mev to 5.2 Mev; thus there is a small gap between our upper limit of 0.48 Mev without observations. In the same figure are shown our $F_{i\infty}$ values for nitrogen gas, which join on to theirs in a very satisfactory manner. Thus, the charge equilibria as established in a beam emergent from celluloid foils, in the forward direction, is within experimental error equal to that set up in nitrogen gas.

[17] Enlarged Figs. 2 to 8, for easier reading of the deduced equilibrium values and cross sections, may be obtained by writing to the authors.

B. Cross Sections

In the case of the cross sections, scattered data on σ_{01}, σ_{10}, and $\sigma_{1\bar{1}}$ are available.[18] The data on σ_{01} and σ_{10} of Eck and Kistemaker cover the Li^7 kinetic energy range 5 to 22.5 kev, and the target gases hydrogen and helium. In the case of σ_{10} in hydrogen there is no significant difference between their results and ours although they used the method of ion collection. At 20 kev their value of σ_{01} agrees exactly with ours (16.5 vs 16×10^{-17} cm^2 per H atom) but they indicate a steeper decline with decreasing kinetic energy than would be indicated by our value of 14 at 10 kev. In the case of the target gas helium there is serious disagreement between their values of σ_{10} and ours. We were unable to find any positive evidence for electron capture by a Li^+ beam in helium gas below 30 kev in energy (see Sec. III-B of this paper), and the Eck and Kistemaker values are above our upper limits. Their values of σ_{01} in helium are 30% lower than ours.[19]

The data of Leviant, Korsunsky, Pivovar, and Podgornyi[2] on σ_{12} in air have been compared to our deductions in nitrogen in Fig. 8. The agreement is not satisfactory in that their values are lower than ours by a factor between 2 and 3. Their estimates of σ_{13} run from

[18] σ_{01}, σ_{10} private communication from Eck and Kistemaker; $\sigma_{1\bar{1}}$ from Fogel, Koslov, Kalmenkov, and Murator, reference 5.

[19] If the Eck and Kistemaker values of σ_{10} for Li^+ in helium gas are correct, the following situation will arise. Since at 20 kev the system is essentially one of two components, we have $F_{0\infty}=\sigma_{10}/(\sigma_{01}+\sigma_{10})$ or with the *EK* cross sections, $F_{0\infty}=0.182$. In the case of H_2 the *EK* cross sections give $F_{0\infty}=0.195$ at the same energy. But other data at similar ion velocities always show a $F_{0\infty}$ in helium much lower than in the more easily ionizable target gases. For instance, a 3-kev hydrogen beam moving in hydrogen gas has $F_{0\infty}=0.897$; in helium gas it has $F_{0\infty}$ only 0.125.

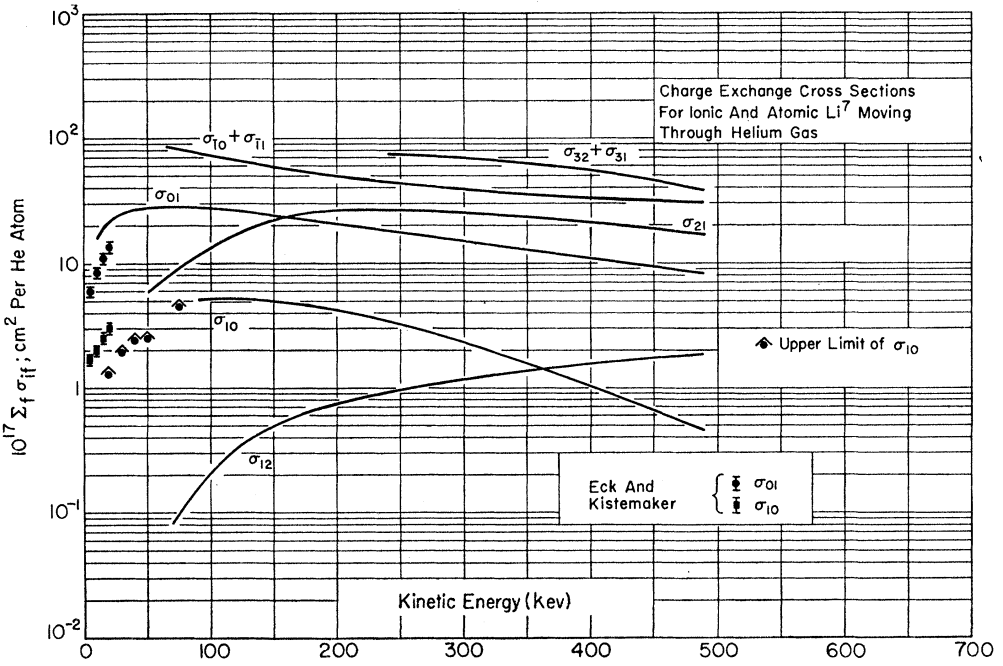

FIG. 7. Charge-changing collision cross sections in helium gas deduced from the sums obtained by direct measurement. Only upper limits to σ_{10} are assigned between 30 and 75 kev. Observations by Eck and Kistemaker are included.

the order of magnitude of 10^{-22} cm^2 at 85 kev to 10^{-19} cm^2 at 250 kev, and justify the assumption we have made in neglecting this cross section in the deductions from our observations in Sec. IV-B of this paper.

The results of Fogel, Koslov, Kalminkov, and Murator on $\sigma_{1\bar{1}}$ in H_2 can be used in connection with our data to deduce values of $\sigma_{0\bar{1}}$ as follows. From Eq. (9) we obtain

$$\sigma_{0\bar{1}}=[F_{\bar{1}\infty}(\sigma_{\bar{1}0}+\sigma_{\bar{1}1})-F_{1\infty}\sigma_{1\bar{1}}]/F_{0\infty}. \quad (15)$$

We need only assume, as we have already indicated, that $(\sigma_{\bar{1}0}+\sigma_{\bar{1}1})$ is essentially $\sum\sigma_{\bar{1}f}$ to conclude that we have measured all the quantities in the right-hand member of Eq. (15) except $\sigma_{1\bar{1}}$. The $\sigma_{1\bar{1}}$ values of Fogel

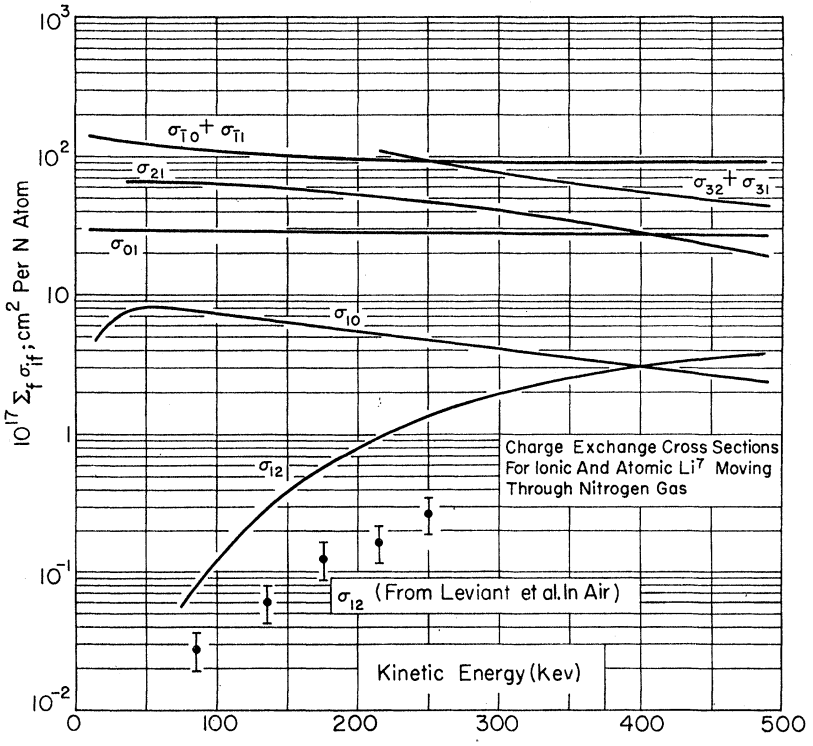

FIG. 8. Charge-changing collision cross sections in nitrogen gas deduced from the sums obtained by direct measurement. Observations of σ_{12} by Leviant *et al.* are also shown.

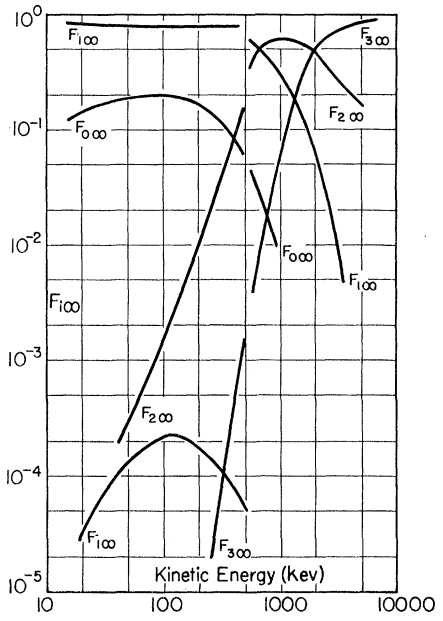

FIG. 9. Results on beam fractions of 15–475 kev lithium ions and atoms moving in nitrogen gas, and those obtained by Teplova *et al.* for a beam with kinetic energies 582 to 5200 kev emerging from celluloid foil.

et al., assumed to be per molecule of target hydrogen, are plotted in Fig. 6 and the $\sigma_{0\bar{1}}$ cross sections deduced from Eq. (15) using them are also plotted. Above 50-kev kinetic energy $\sigma_{\bar{1}1}$ is completely negligible compared to the observed $\sum\sigma_{\bar{1}f}$ and the subtractive term in the right-hand member of Eq. (15) can be dropped.

VI. OBSERVATIONS AND CONCLUSIONS

A. Comments on the Equilibrium Fractions $F_{i\infty}$

The maximum yield of Li^- through charge equilibration of a lithium beam in a gas seems to be about $F_{\bar{1}\infty}=3\times10^{-4}$, attainable in H_2, He, propane, or N_2O. But it is a striking feature, exhibited in Fig. 5 that this yield is attained at a much lower kinetic energy in C_3H_8 and N_2O than in H_2, He, and nitrogen. Thus in designing an ion source for the production of Li^- by equilibration in a gas, C_3H_8 and N_2O would deserve serious consideration as the equilibrating gases because at the comparatively low kinetic energy of 40 kev they can produce a yield of Li^- only attainable at several hundred kilovolts in the elementary gases. This behavior is presumably connected with the relatively low ionization potentials of the complex gases.

Another remarkable feature is the relatively very high $F_{2\infty}$ in helium gas at the lower kinetic energies. Thus for a 60-kev Li^7 beam, $F_{2\infty}=1.3\times10^{-4}$ and 4.7×10^{-4} in the target gases H_2 and N_2, respectively, but 9.4×10^{-3} in helium. Helium is, at this kinetic energy, 72 times as effective as hydrogen in stripping a Li^+ beam. A study of the cross sections as shown in Figs. 6 to 8 reveals that this effect is not due to an abnormality in the stripping cross section σ_{12} in helium, but due to helium's abnormally low σ_{21}. Thus Li^{++} is initially produced in helium gas from Li^+ at a probability per collision which is not anomalous, but because of the low σ_{21} in helium, accumulates in the beam as the pressure in the converter cell is increased. In fact, the anomalously high $F_{2\infty}$ in helium is attained at a significantly higher converter cell pressure than required to attain charge equilibrium using H_2 or N_2. At higher lithium kinetic energies the anomalous efficiency of helium declines, and at 475 kev $F_{2\infty}$ is slightly greater in nitrogen than in helium (0.13 vs 0.10) and is comparable in hydrogen (0.07). Thus, the chemical nature of the target gas shows up mainly at the lower kinetic energies, as has already been seen in the formation of Li^-.

B. Electron Capture by Isoelectronic Beam Constituents Moving with the Same Velocity in Different Target Gases

The data on lithium presented here, plus previous data accumulated on hydrogen and helium beams, have made possible a kind of empirical approach to the discovery of the laws of charge changing collision. For instance, consider the bare nuclei H^+, He^{++}, and Li^{+++}. If one compares their electron capture probabilities,

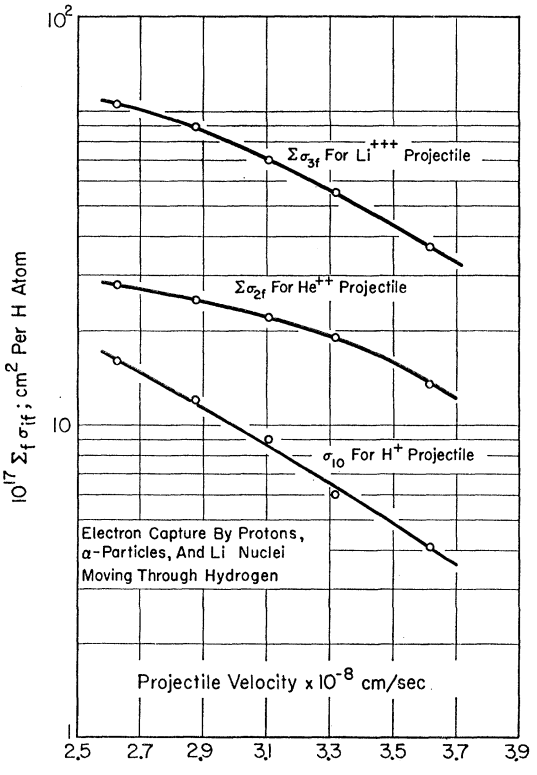

FIG. 10. Electron capture cross sections for protons, α particles, and Li^7 nuclei moving through hydrogen gas, compared at the same velocities. At the higher velocities the cross sections are approximately in the ratios of the square of the nuclear charge of the projectile.

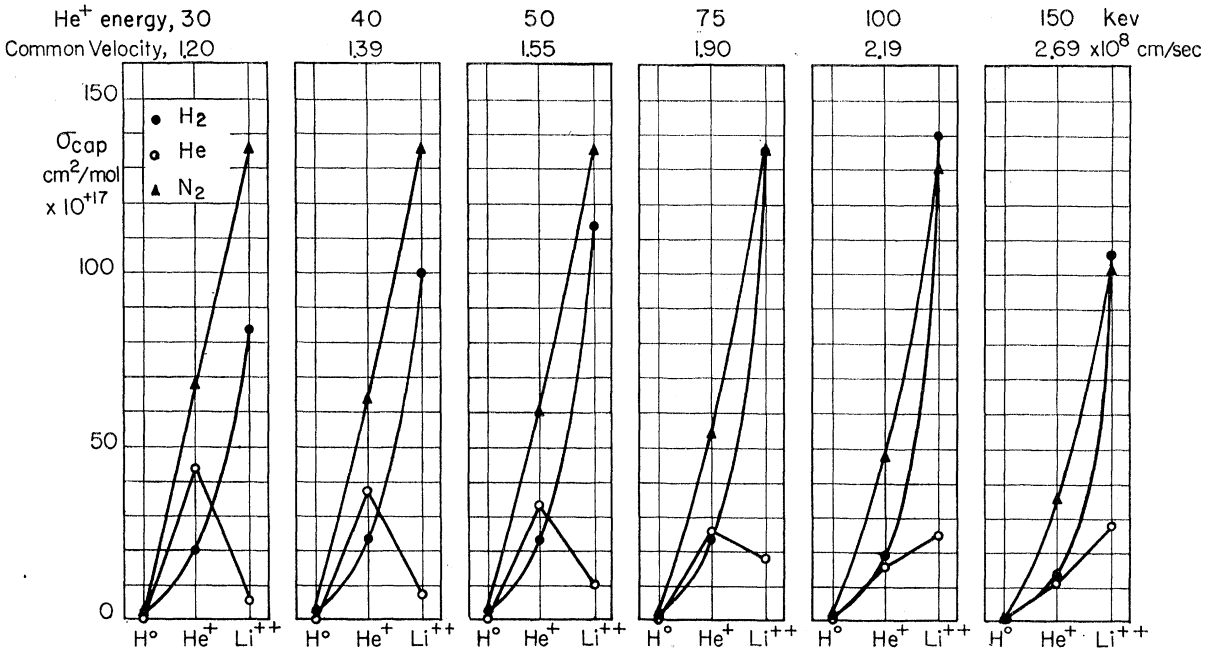

FIG. 11. Comparison of the charge-changing collision probabilities of projectile atoms and ions of the same electronic structure and the same translational velocity through the gases H_2, He, and N_2. The isoelectronic structure is the nucleus plus one s electron. The anomalously large cross section for the resonant reaction $He(He^+, He)He^+$ at low velocities is clearly indicated.

moving with the same velocity through the same target gas, the significant differences should be those due to the monotonically increasing nuclear charge. If we study their behavior in hydrogen gas, we have our best (but poor in the case of H^+ in H_2) approximation to capture by a projectile of high electron affinity from a target where electrons are comparably or more loosely bound. Furthermore, the work of Allison[19] indicates that double electron capture is unlikely in H_2, because of the extended nature of the H_2 molecule. Figure 10 shows the electron capture cross sections of H^+, He^{++}, and Li^{+++} in H_2 gas, such that common abscissas mean common velocities. The energy range shown for lithium is from 250 to 475 kev. At the higher velocities it seems clear that the cross-section ratios are approaching the ratios of Z^2, namely 9:4:1. Such a dependence on Z^2 is indicated in the theory.[20] In the case of electron capture by these bare nuclei traversing He and N_2 the cross sections increase with the Z of the moving nucleus but are not in the simple ratio of Z^2. In particular, the ratio $|\sum\sigma_{2f}|_\alpha/|\sigma_{10}|_p \sim 15.5/8$, and, at the common velocity 1.36×10^8 cm/sec for α particles and protons moving through helium gas, is less than 4. The effect of the resonant simultaneous capture of 2 electrons by the α particle is not obvious.

Another comparison of the behavior of isoelectronic projectiles may be made by looking at the electron capture by H^0, He^+, and Li^{++} traversing various gases at the same velocity. The configuration of the projectile here is the nucleus accompanied by one atomic electron in an S orbit. The capture cross sections being compared are, $\sigma_{0\bar{1}}$, σ_{10}, σ_{21} for H^0, He^+, and Li^{++}, respectively, and the situation is illustrated in Fig. 11. Studying the figure from left to right, the first panel exhibits the properties of isoelectronic $1s$ configurations moving with the common velocity 1.20×10^8 cm/sec. The points shown with solid triangles represent the electron capture cross sections of these configurations, in the order (from left to right) H^0, He^+, Li^{++}, in the target gas nitrogen. (The solid lines connecting the points are, in this representation, only to guide the eye; there are no intermediate points.) Values of σ are given per molecule of target gas. As we see, there is a monotonic increase in the capture probability in nitrogen as the electron affinity of the isoelectronic configuration increases (0.73, 24.5, and 75 ev, respectively). The points in solid circles similarly apply to the target gas H_2, and we see a similar monotonic increase from 2.25 through 20 to 84×10^{-17} cm^2 from H^0 to Li^{++} projectiles. The open-circle points refer to the target gas helium, and here we see the large anomaly in the resonant case of He^+ moving in helium gas; the observed value for $He^0(He^+,He^0)\,He^+$ is 43×10^{-17} cm^2, about 15 times larger than would be predicted by monotonic interpolation between the projectiles H^0 and Li^{++}.

As we take successive panels from left to right in Fig. 11 the situation is exhibited at higher and higher velocities. The anomaly is obviously decreasing and at a velocity of 2.7×10^8 cm/sec the sequence of σ's in

[20] See J. D. Jackson and H. Schiff, Phys. Rev. **89**, 359 (1953), Eqs. (9) and (15), p. 361.

helium gas approximates the nonresonant cases of the target gases H_2 and N_2.

C. Theoretical Predictions of Maxima in Charge-Changing Cross Sections vs Kinetic Energy

Some of the cross-section curves obtained in the present work show maxima which can be compared with the general predictions of Massey's "adiabatic hypothesis".[21] Basically this hypothesis deduces the general behavior of the cross-section curves by comparing the relative magnitude of the transition time and the duration of the collision. In this way it results that the principal parameter is

$$a|\Delta E|/hv, \tag{16}$$

where "a" is a length of the order of atomic dimensions, ΔE is the change of internal energy of the particles when they interact, h is Planck's constant, and v is the velocity of approach of the particles. When v is small $a|\Delta E|/hv \gg 1$ and the probability increases rapidly with the velocity and it is expected that the cross section reaches a maximum for $a|\Delta E|/hv_{\max} \approx 1$. At higher energies the probability of this type of interaction decreases.

It is found that the length "a" is approximately constant for a variety of processes. For charge-exchange processes (capture of one electron by projectile or target), or ionization or excitation of the target by a positive ion projectile, the mean value[22] is 8A. Fogel *et al.*[23] find $a \approx 3$A for processes of reverse neutralization (capture of one electron by a neutral atom) and $a \approx 1.5$A for capture of two electrons.

Our curves show broad maxima which only allow an estimate of the order of magnitude of "a" [Eq. (16)]. If we assume we are dealing only with transitions from and to the ground state in target and projectile, we find "a" depends on the type of reaction. Roughly the ionization of the atomic projectile in H_2, He, N_2 (σ_{01}) shows an "a" of about 10A, while in H_2 and He σ_{10} indicates 5A, and σ_{21}, 1.7A. It is a surprising fact that, within the uncertainty of our experiments we are unable to see maxima for σ_{01} or σ_{21} in N_2 gas.

Fan[24] has emphasized the important role played in the charge-exchange process by the perturbation terms in the Hamiltonian which correspond to the Coulomb interaction of projectile and target.

In his treatment, application of the laws of conservation of energy and momentum to charge-changing collisions shows that in the general case there is a minimum but finite momentum transfer to the target particle. This corresponds to a diffraction of the incident particle waves through an angle

$$\phi \sim \tfrac{1}{2}(|\Delta E|/E - m/M),$$

where ΔE is the difference in binding energies of the electron in the projectile and in the target, E is the projectile energy, and m and M are the masses of electron and projectile, respectively.

A maximum impact parameter and cross section will be associated with a minimum interference effect and therefore for a charge-changing reaction the maximum should be found at projectile energy

$$E_M = |\Delta E| M/m.$$

We have compared the occurrence of our maxima with this criterion and found that the maxima are systematically at lower energies than predicted. This displacement is in the range of 40 to 100 kev, except for σ_{21} where it is much greater. However, in this latter case the difference would not be so large if capture in excited states were considered.

ACKNOWLEDGMENTS

Our thanks are due to John Erwood for maintenance of the apparatus and assistance in taking data. Minao Kamegai prepared the emitting lithium aluminum silicates. Marshall Huberman assisted in taking some of the readings.

[21] H. S. W. Massey and E. H. S. Burhop, *Electronic and Ionic Impact Phenomena* (Oxford University Press, New York, 1952), Chap. VIII.

[22] J. B. Hasted (to be published).

[23] Ya. M. Fogel, R. V. Mitin, V. F. Kozlov, and N. D. Romachko, J. Exptl. Theoret. Phys. (U.S.S.R.) **35**, 565 (1958) [translation: Soviet Phys.-JETP **8**, 390 (1959)]; see also Ya. M. Fogel, V. A. Ankundinov, and D. V. Pilipenko, J. Exptl. Theoret. Phys. (U.S.S.R.) **35**, 868 (1958) [translation: Soviet Phys.-JETP **8**, 601 (1959)].

[24] C. Y. Fan's ideas as originally expressed [Phys. Rev. **103**, 1740 (1956)], have been subsequently elaborated by him and transmitted to us through private communication.